

Experimental Technique for Studying Aerosols of Lyophilized Bacteria

CHRISTOPHER S. COX,¹ JOHN S. DERR, JR., EUGENE G. FLURIE, AND ROGER C. RODERICK

Biological Sciences Laboratories, Physical Science Division, Fort Detrick, Frederick, Maryland 21701

Received for publication 10 August 1970

An experimental technique is presented for studying aerosols generated from lyophilized bacteria by using *Escherichia coli* B, *Bacillus subtilis* var. *niger*, *Enterobacter aerogenes*, and *Pasteurella tularensis*. An aerosol generator capable of creating fine particle aerosols of small quantities (10 mg) of lyophilized powder under controlled conditions of exposure to the atmosphere is described. The physical properties of the aerosols are investigated as to the distribution of number of aerosol particles with particle size as well as to the distribution of number of bacteria with particle size. Biologically unstable vegetative cells were quantitated physically by using ¹⁴C and Europium chelate stain as tracers, whereas the stable heat-shocked *B. subtilis* spores were assayed biologically. The physical persistence of the lyophilized *B. subtilis* aerosol is investigated as a function of size of spore-containing particles. The experimental result that physical persistence of the aerosol in a closed aerosol chamber increases as particle size is decreased is satisfactorily explained on the bases of electrostatic, gravitational, inertial, and diffusion forces operating to remove particles from the particular aerosol system. The net effect of these various forces is to provide, after a short time interval in the system (about 2 min), an aerosol of fine particles with enhanced physical stability. The dependence of physical stability of the aerosol on the species of organism and the nature of the suspending medium for lyophilization is indicated. Also, limitations and general applicability of both the technique and results are discussed.

A recent review of microbial aerosols (1) clearly concluded that most work had been performed with wet-generated aerosols. The present paper presents and analyzes an experimental technique for the laboratory study of aerosols generated from lyophilized bacteria under conditions such that the dry material is minimally exposed to uncontrolled atmospheres. Such work is important to an understanding of microbial aerosols since wet and dry disseminated aerosols are not equivalent (2). Application of the methodology to studies of aerosols of dry inert particulate solids is also possible.

MATERIALS AND METHODS

Evaluation of the experimental technique for studying lyophilized bacteria in aerosols involved use of *Escherichia coli* B and heat-shocked spores of *Bacillus subtilis* var. *niger* as the major test organisms. *Enterobacter aerogenes* and *Pasteurella tularensis* were also studied, but in less detail. Distilled-water-washed 16-hr cultures of *E. coli* B and distilled-water-washed spores were freeze-dried in a "Waffle-iron" freeze-

drier (9). One characteristic of the freeze-drier was that 15-ml serum bottles were used to contain the freeze-dried material. The serum bottles, after freeze-drying, were sealed in vacuo with serum caps. The aerosol generator, designed by E. G. Flurie and R. C. Roderick after a basic concept by G. D. Gordon, incorporates the lyophilizing serum bottle as an integral part. Hence, exposure of the freeze-dried material to the atmosphere before dissemination is minimized, whereas lyophilized material remains sealed under vacuum in the serum bottles until they are pressure-equilibrated with a preselected gas and inserted into the aerosol generator at the time of dissemination.

E. coli B tagged by ¹⁴C (2) or by Europium chelate stain (8) were similarly prepared as freeze-dried powders. Particle-size analyses of aerosols were obtained by using a Cascade Impactor (5), a modified Andersen sampler (6), and Micromerograph manufactured by The Sharples Corp., Bridgeport, Pa. The all-glass impinger (7) was also used for aerosol recovery measurements, both physical and viable. The aerosol-testing chamber was a 75-liter stainless-steel drum (4) maintained in a room at 26.5 ± 0.2 C. For biological assay of microorganisms, standard plating, incubation, and colony-counting procedures were followed.

The aerosol generator for lyophilized bacteria is shown schematically in Fig. 1. It is a relatively simple

¹ Present address: Naval Biological Laboratory, Naval Supply Center, Oakland, Calif. 94625

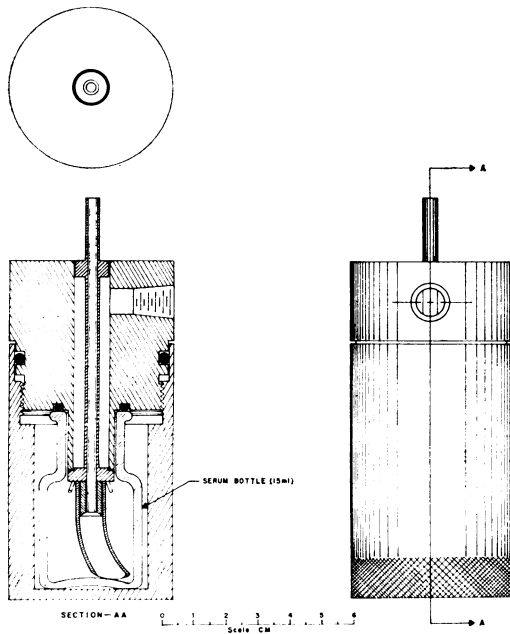


FIG. 1. Aerosol generator for lyophilized bacteria.

pneumatic device incorporating a high-pressure chamber with four jets tangential to the outlet tube oriented 45° downward from the horizontal plane and 20° outward from the vertical planes passing through the points of tangency and an outlet jet. The tangential jets consist of hypodermic needle tubing (no. 20 gauge). There are no moving parts. High-pressure gas (nominally nitrogen, but selected at discretion) expands from the four tangential jets and forms a vortex which causes surface turbulence phenomena. When gas is introduced into the 15-ml serum bottle via the four inlet jets, angular momentum is imparted to the gas above the powder (Fig. 2). This rotation, coupled with the effect of the outlet jet, forms a vortex inside the serum bottle violent enough to disturb the powder which is loosened by surface turbulence and transported by the vortex to the outlet. As particles move from the surface of the bed of powder to the exit, centrifugal action of the vortex forces heavier particles away from the center. If the particles are heavy enough, they will not pass through the outlet but will move out to the walls and return to the surface of the powder. Large agglomerated particles will be retained in the serum bottle and continue to collide with each other and with the walls until sufficiently reduced in size to permit escape through the outlet. This small-particle-selection phenomenon is an important feature of the vortex-type aerosol generator. Whereas few large particles appear in the aerosol due to the size-selective process, some fine particles do remain in the aerosol generator. Residue in the disseminator results both from cohesion on the surface of some fine particles whose forces are stronger than the disruptive forces of the vortex, as well as from the size-selective inertial effects of large particles. For a given

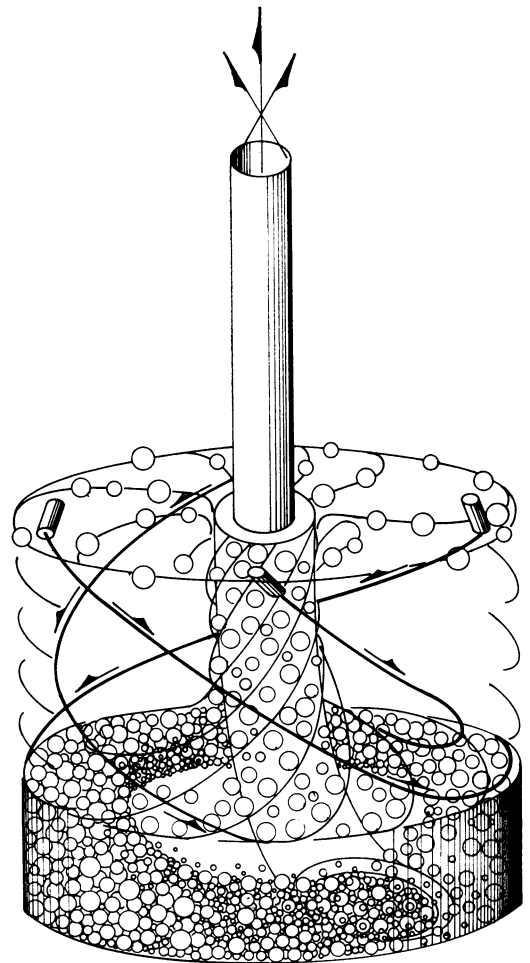


FIG. 2. Schematic aerosol generator operating mode.

operating condition of the generator, the amount of residue will depend upon the nature of the lyophilized powder.

In practice, the aerosol generator is attached to a cylinder of dry nitrogen via a reducing valve and a solenoid valve. The working pressure is 90 psig with a corresponding gas flow rate of 2.5 standard cubic feet per minute (SCFM). The relationship between pressure and flow rate for the aerosol generator used in this study is shown in Fig. 3. Each device should be calibrated for its flow rate-pressure relation and checked periodically to preclude clogging of the critical flow tangential jets.

The nominal net fill of lyophilized powder is about 10 mg obtained by lyophilizing 1-ml samples of bacterial suspension. The total number of bacteria per gram of dried powder is about 5×10^{12} , with viable percentages ranging between 20 and 100%, depending on the bacterial species and suspending medium for the lyophilization process.

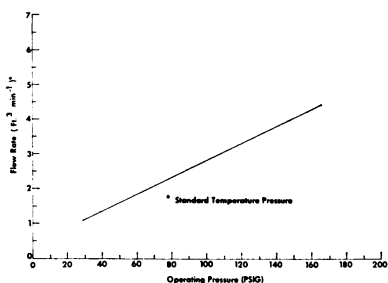


FIG. 3. Gas flow rate as a function of operating pressure for the aerosol generator.

By using the above values for operating pressure and net fill weight, test aerosols are generated in a few seconds. The aerosol generator can be operated in both vertical and horizontal positions.

RESULTS AND DISCUSSION

Aerosols of heat-shocked lyophilized *B. subtilis* var. *niger* spores showed no losses in viability under the conditions of the experiment. Consequently, the biological measure of the normalized distribution of numbers of viable cells in the aerosols as a function of size of aerosol particle containing those cells is theoretically identical to the physical measure of the normalized distribution of mass of cells in the aerosol as a function of size of aerosol particles. The former distribution is referred to as a "viability size distribution" of the aerosol, and the latter distribution is referred to as a "mass-size distribution" of the aerosol. Where there is no viable loss, or where viable loss is independent of aerosol particle size, these normalized distributions are identical. This identity is shown by the following equation:

$$m(d) = n_b(d) \frac{\pi}{6} \times \rho_b \times d_b^3 \text{ where } m(d) = \text{mass}$$

of aerosol particle with diameter d , $n_b(d)$ = number of bacteria in aerosol particle of diameter d , ρ_b = density of a bacterial cell, d_b = equivalent spherical diameter of a bacterial cell.

The particle size distribution of the *B. subtilis* aerosol as produced by the aerosol generator was measured by dynamic sampling of the aerosol efflux directly out of the aerosol generator during its operation with a Cascade Impactor (5) manufactured by C. F. Casella & Co., London. The sampling technique involved the use of agar-coated slides to provide for efficient physical sampling and to permit recovery of spores by a washing procedure for viable assay. A cumulative viability-size distribution, which for the experimental *B. subtilis* aerosol is equivalent to the cumulative aerosol mass-size distribution, is then constructed by using the Cascade Impactor cali-

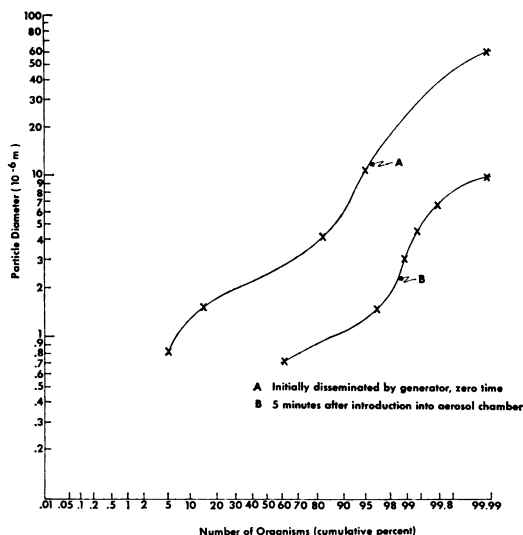


FIG. 4. Cumulative aerosol viability-size distributions of lyophilized *B. subtilis* var. *niger* aerosols, equivalent to aerosol mass-size distributions.

bration, relating impaction stage and its associated equivalent aerosol particle size. Minimum aerosol particle size and maximum particle size were obtained by observation in an optical microscope. These observations disclosed that single spores constituted the minimum size present and aggregates of approximately $60 \mu\text{m}$ constituted the largest particles present, characterizing the end points on the distribution curve. These size data normalized to 100% are given in Fig. 4A. About 95% of the generated aerosol is comprised of particles whose sizes are consistent with requirements for collection in the impinger (7).

The viability-size distribution of the *B. subtilis* aerosol generated by direct coupling of the aerosol generator to the rotating drum and allowed to age for 5 min in the drum at 85% relative humidity and at 26.5°C was obtained with a modified Andersen sampler (6). These data, normalized to 100%, are shown in Fig. 4B. Both distributions of Fig. 4A and 4B are equivalent to the aerosol mass-size distribution, with particle size expressed in terms of the diameter of a spherical particle having equivalent aerodynamic drag characteristics as the particle being sampled.

It is to be noted, by comparing the normalized size distribution of the initially disseminated aerosol (Fig. 4A) with the normalized size distribution of the aerosol after 5 min in the rotating drum (Fig. 4B) that a shift to smaller sizes has occurred as a result of the "aging" process. The net combined effect of the generator (to initially produce an aerosol) and the rotating drum (to

further modify the aerosol) is to provide a physically stable aerosol of fine particles for subsequent study and evaluation.

However, in addition to the distribution of sizes of particles in an experimental aerosol, the concentration of bacteria is a factor of prime importance, particularly in experiments requiring biochemical analyses of recovered aerosol samples, or studies involving the control of aerosol dosages for measurement of host response. With the *B. subtilis* aerosols, it was found that of the initial number of spores in powder form resulting from the lyophilization process and before dissemination (nominal weight of 10 mg), 2% was in aerosol form in the rotating chamber 5 min after dissemination as an aerosol.

Because of desirability of obtaining maximum recovery in aerosol form of the lyophilized material, particularly in the case of the small quantities associated with the current studies, an analysis of the nature of the low recovery in the aerosol was made. The loci of the unaccounted 98% of *B. subtilis* spores initially lyophilized, and not appearing in the aerosol after 5 min in the drum, could be assigned a priori as either: (i) residue in the serum bottle where drying occurred; (ii) residue in the disseminator caused by hang-up on generator surfaces; (iii) losses to the walls of the aerosol chamber during the process of aerosol dissemination and as the aerosol aged in the 5-min interval prior to the aerosol sample. By using a combination of gravimetric techniques and plating techniques, residues in (i) the serum bottle, and (ii) the generator were measured directly. Although results were somewhat variable from experiment to experiment, significant mean values were obtained: (i) serum bottle residue, 46% of starting material; (ii) disseminator loss, 29% of starting material. These values, coupled with the aerosol recovery at 5 min of 2% of the starting material, enabled the losses associated with chamber per se, (during dissemination and as a result of cloud aging) to be calculated, i.e., (iii) chamber loss, 23% of the starting material.

The relationship between particle size and dissemination efficiency of the aerosol generator and the tacit relationship between particle sizes and persistence of the aerosol as it involves gravitational sedimentation necessitated an investigation of the physical dispersion of the total lyophilized sample. The extent to which large aggregates of spores were present in the powder and how such aggregates could withstand dissemination or promote aerosol physical decay was determined. The size characteristics were obtained by using the Sharples Micromerograph (3) in which the total sample of lyophilized material is both efficiently disseminated and sampled on a mass

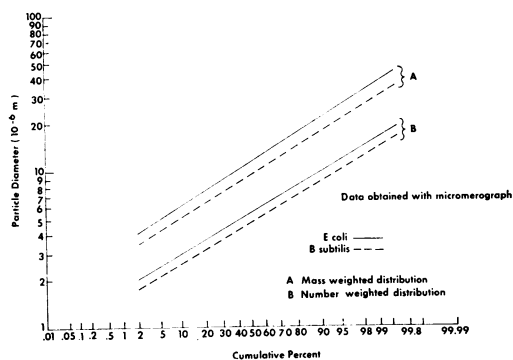


FIG. 5. Control aerosol mass-size distributions and aerosol particle-number distributions, as a function of particle size, of lyophilized *B. subtilis* var. *niger* and *E. coli* aerosols.

weighted basis. The mass-size distribution of aerosols of lyophilized *B. subtilis* as well as *E. coli* are given in Fig. 5A on a cumulative per cent basis. Also shown is the transformation from the mass-size distribution of the aerosols to the particle number-size distributions. This transformation is required for any consideration involving numbers of aerosol particles containing bacteria in contradistinction to numbers of bacteria per se, such as the distribution of particles in size-discriminating samplers. An example would be a requirement for knowledge of the distribution and number of potential infection sites in the lung. The transformation is obtained graphically for each size class increment by: $f(m) = f(n)\bar{d}^3$ where $f(m)$ = particle mass-size distribution function or viability-size distribution function, $f(n)$ = particle number-size distribution function, \bar{d} = equivalent spherical particle diameter for the size increment. These measured size distribution data are entirely consistent with a theoretical model for size distributions of aerosols of dry mono-disperse particles developed by Derr (3). The model predicts a quasi-logarithmic size distribution having a geometric standard deviation of 1.6 ± 0.1 and a ratio of mass median diameter to particle number median diameter of 1.95. However, maximum sizes present in the aerosol depend on the nature of the powder and aerodynamic characteristics of the generator (3).

A conclusion drawn from the Micromerograph data is that aggregates contribute both to residue in the serum bottle as well as to physical losses in the generator. A comparison of the mass distribution curves for *B. subtilis* in differential form (Fig. 6) shows a concomitant progressive decrease in median particle size and size range of material in its various states, i.e., after lyophilization, after dissemination, and after aerosol aging. Data

were normalized to the total quantity in each of these states as 100%. A replotting of the mass-particle size data of *B. subtilis*, but normalizing the data to the initial amount of material lyophilized, shows both the particle size shift as well as the loss of material to those respective states as the material is disseminated and subsequently decays in aerosol form (Fig. 7). A major change in the mass weighted distribution occurs in the larger size fractions, i.e., particles larger than 10 μm in diameter are not efficiently disseminated as an aerosol, and those larger than 2 μm in diameter disappear from the aerosol as a result of the process of introducing the aerosol into the drum and subsequent aerosol physical decay in the drum as the cloud ages.

For those studies involving characteristics of bacteria which are time dependent in the aerosol form, obtaining a physically stable aerosol in the aerosol test chamber is an essential experimental requirement. Irrespective of the nature of the particle size distribution associated with the initially disseminated aerosols (a function of the nature of the test material and the particular disseminator used), processes will occur to modify further the distribution as a result of the interaction of the disseminated aerosol and the aerosol chamber. The physical stability of the aerosol will depend upon such processes. To clarify the nature of mechanisms operating in any test chamber, a theoretical model to predict probabilities of persistence of particles in the test facility as a function of time has been formulated and applied to the conditions of this study. Physical losses associated with aerosol dissemination and storage can be attributed to the following four mechanisms in isothermal, closed aerosol chambers. (1) Electrostatic precipitation to chamber

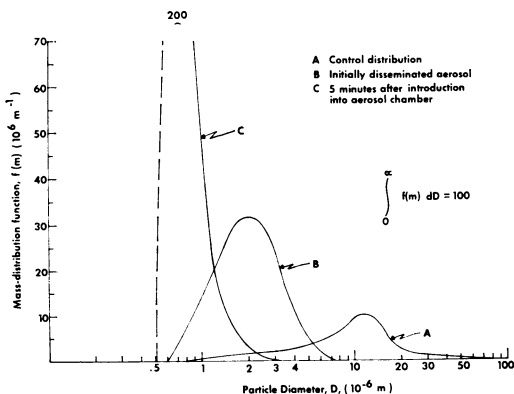


FIG. 6. Effect of generator and aerosol chamber on normalized mass-size distribution function of lyophilized *B. subtilis* var. *niger* aerosols.

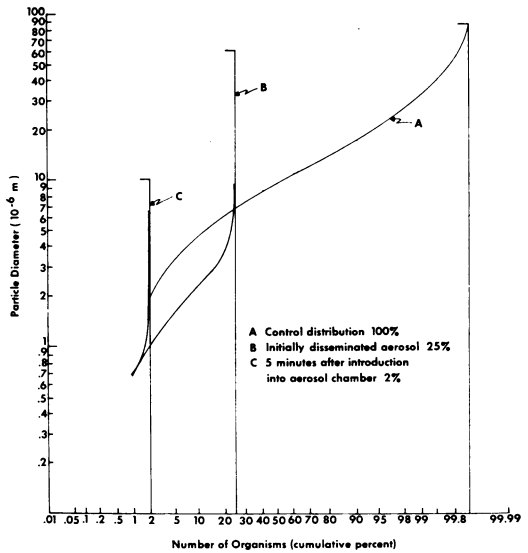


FIG. 7. Effect of generator and aerosol chamber on both recovery of lyophilized *B. subtilis* var. *niger* spores and the related particle size distribution.

walls due to the presence of image charges of aerosol particles for chambers whose walls are conductors. This effect is diffusion-dependent. (2) Inertial impaction due to the presence of bent streamlines and impaction surfaces. It is particularly important in the aerosol dissemination phase. (3) Gravitational settling, an effect always present in any chamber design and a maximum for tranquil, nonstirred aerosols. (4) Brownian diffusion. (Thermal precipitation, a special case of diffusion loss, is not applicable in an isothermal experimental process such as the present one, but can be important where chamber surfaces are colder than the cloud environment.)

The probability of persistence of particles for each of the above attrition effects can be approximated by the following equations. The Stokes-Cunningham slip correction factor is negligibly small for particles under consideration, and is ignored.

(1) Electrostatic precipitation:

$$P_e = [2kT / (K_1 K_2 X^3)]^{1/2} (1/d^2) (n_c/n_o) \quad (1)$$

where k = Boltzmann constant; T = absolute temperature; K_2 = constant for a given aerosol, relating particle charge to particle area, having units of stat coulombs per cm^2 in the CGS system of units and being dependent on the properties of powder and dissemination system; K_1 = Coulomb force constant, unity in the CGS system of units; X = characteristic electrostatic trapping distance measured from chamber surfaces, system-de-

pendent, probably of the order of the boundary layer thickness; d = aerosol particle diameter; and n_c/n_o = ratio of number of charged particles of either sign to the total number of particles at X .

(2) Inertial impaction:

$$P_1 = (K_3 18\eta\bar{R})/(\rho\bar{V}_s d^2) \quad (2)$$

where K_3 = factor of proportionality between impaction probability and the ratio of viscous forces to centrifugal forces acting on a particle, system-dependent; η = viscosity of gaseous medium; \bar{V}_s = characteristic stream velocity, system dependent; \bar{R} = characteristic streamline radius of curvature, system-dependent; ρ = density of particle; and d = aerosol particle diameter.

(3) Gravitational sedimentation:

$$P_g = 1 - (\rho g d^2 t)/(18\eta H) \quad (3)$$

where t = aerosol age, H = effective chamber height, η = viscosity of medium, ρ = particle density, d = particle diameter, and g = gravitational acceleration.

(4) Brownian diffusion:

$$P_D = 1 - (2kTt)/(3\pi\eta d R_o^2) \quad (4)$$

where k = Boltzmann constant, T = absolute temperature, t = aerosol age, η = viscosity of medium, R_o = chamber half-width (radius for a cylindrical chamber), and d = particle diameter.

Equal exposure of all particles in time to electrostatic and inertial effects is assumed. These effects largely result from the dynamic interaction of the aerosol particles upon dissemination and with the aerosol ducting and chamber surfaces.

Since the expressed probabilities of physical persistence are independently operating, the net probability of the aerosol to persist in the system is expressed by:

$$P_P = P_e \times P_1 \times P_g \times P_D \quad (5)$$

For a given system, i.e., with powder, disseminator, disseminator operating conditions, and chamber defined, such as the present system with *B. subtilis* powder, the net probability of aerosol persistence can be expressed in terms of system constants, particle size, and time. An effect, not considered here, of rotating the drum about an axis perpendicular to gravity would be to increase further physical persistence over extended periods of time (4).

Rewriting equation (5):

$$P_P = (A/d^2)(B/d^2)(1 - Cd^2t)(1 - Dt/d) \quad (6)$$

where $A = (n_c/n_o)[(2kT)/(K_1 K_2^2 X^2)]^{1/2}$ and is an undetermined system constant; $B = (K_3 18\eta\bar{R})/$

(ρV_s) and is an undetermined system constant; $C = (\rho g)/(18\eta H)$ and is known; and $D = (2kT)/(3\pi\eta R_o^2)$ and is known. The known constants can be computed for the *B. subtilis* aerosol and the aerosol chamber dimensions under consideration as:

$$\begin{aligned} C &= (1.3 \text{ g per cm}^3 \times 980 \text{ cm per sec}^2) / \\ &\quad (18 \times 1.84 \times 10^{-4} \times \text{g per cm per} \\ &\quad \text{sec} \times 60 \text{ cm}) \\ &= 5.05 \times 10^8 \text{ per cm}^2 \text{ per sec.} \\ D &= (2 \times 1.38 \times 10^{-16} \text{ g} \times \text{cm}^2 \text{ per sec}^2 \\ &\quad \text{per } ^\circ\text{K} \times 300^\circ\text{K}) / (3 \times 3.14 \times \\ &\quad 1.84 \times 10^{-4} \text{ g per cm per sec} \times \\ &\quad 900 \text{ cm}^2) \\ &= 5.3 \times 10^{-14} \times \text{cm per sec.} \end{aligned}$$

For the *B. subtilis* aerosol having a cloud age of 5 min, the Brownian diffusion loss is demonstrated to be negligible. For $d = 10^{-4}$ cm and $t = 300$ sec: $Dt/d = 1.5 \times 10^{-7}$; therefore, $P_D = 1$. Hence, the probability of physical persistence of particles as expressed by equation (6) can be rewritten as a function of time and size, involving a single system constant.

$$P_P = G[(1/d^4) - (Ct/d^2)] \quad (7)$$

where $G = A$ times B and is an undetermined constant for the system, cm^4 ; $C = 5.05 \times 10^8$ per cm^2 per sec; t = cloud age (seconds); d = particle diameter (centimeters).

The indeterminant nature of this constant, G , precludes calculation of an *absolute* physical persistence probability distribution function, but normalization does permit the *relative* physical persistence probability as a function of particle sizes to be calculated.

An *absolute* experimental determination of the physical persistence probability is possible by using the data of Fig. 4 renormalized to the initial number of organisms originally disseminated as an aerosol. This renormalization on a per cent basis is shown in Fig. 7. For each corresponding particle size class in the two distributions, the ratio of numbers of bacteria physically present in the aerosol after 5 min to the initial number disseminated in the corresponding size class determines the value of the absolute persistence probability distribution function in incremental form. From this, a *relative* experimental probability distribution as a function of particle size can be calculated and compared with the *relative* prediction of the theoretical model. This comparison is shown in Fig. 8 where unity has been arbitrarily set for the value of the function corresponding to a particle size of 0.9 μm diameter. (The absolute experimental value of the persistence probability for this particle size was 0.32, leading to an

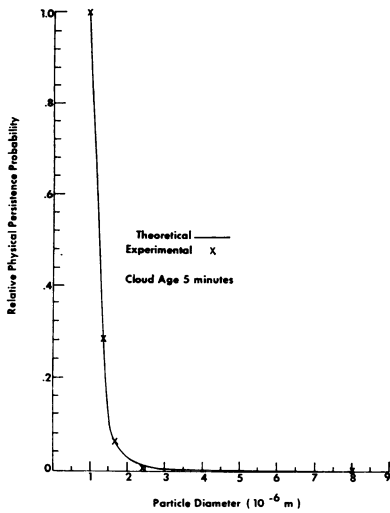


FIG. 8. Relative physical persistence of aerosol particles in the aerosol chamber as a function of particle size, as measured and as theoretically predicted.

experimentally derived value of $G = 2.1 \times 10^{-17} \times \text{cm}^4$ for the particular system under discussion.) The fit between theory and experiment is perhaps unjustifiably good because of the simplifications built into the theoretical model. The theoretical and experimental agreement does serve, however, to confirm in a qualitative sense the physical rationale applied to describe the physical stability of the *B. subtilis* aerosol. It further demonstrates that associated with significant physical losses of bacterial spores from the aerosol state, a residual small percentage is retained in stable form, primarily as single spores.

As indicated in the above discussion of the physical stability of the *B. subtilis* aerosol, physical characteristics, including size distribution and electrostatic charge properties, are dependent on the nature of the powder. For experiments using aerosols of bacteria undergoing biological decay, it is necessary to use a tracer to obtain a measure of total physical recovery, which together with a viable recovery enables a calculation of the biological decay rate to be measured (1). Initially, mixtures of *E. coli* B and *B. subtilis* var. *niger* spores were used, the latter acting as the tracer. It soon became evident that these two organisms did not behave the same physically in the aerosol chamber, despite a similarity of particle size properties of the lyophilized product as determined by using the Micromerograph (Fig. 5). Hence, erroneous viability results would be obtained with this tracer technique in the system. To determine the pattern of fallout in the drum of *E. coli* B, settling slides were not used as they were for *B.*

subtilis var. *niger* spores. Viability losses of *E. coli* B would prevent colony counts on nutrient agar surfaces from being used to compute numbers of *E. coli* B on settling slides. Instead, *E. coli* B stained with Europium chelate (8), which when excited with ultraviolet light fluoresces with red light, was used to determine the physical fallout pattern of *E. coli* B. By means of this technique, it was evident that, unlike *B. subtilis* var. *niger* spores, *E. coli* B did not undergo pronounced electrostatic physical loss in the drum but rather in the aerosol-generation portion of the system including duct surfaces leading into the drum. The resulting aerosol in the drum was therefore more physically stable from the electrostatic point of view. Hence, the differences in physical behavior are accounted for. As an alternative to using *B. subtilis* var. *niger* spores as tracer (1), *E. coli* B tagged with ¹⁴C (2) has been successfully used.

To further demonstrate that the nature of the dried material significantly affects aerosolization characteristics, a comparison among several organisms, physically traced and suspended in various ways, lyophilized, and disseminated as an aerosol by using the presently described technique, is presented in Table 1. The values given are for that portion of lyophilized bacteria initially present in the serum bottle prior to dissemination which has physically persisted for 2 min as an aerosol after dissemination into the rotating drum. Differences in physical behavior are apparent from the variability of recovery. The aerosol of greatest initial physical stability and dissemination efficiency based on these measurements at a cloud age of 2 min would appear to be vegetative cells lyophilized from distilled water and traced with ¹⁴C. The apparent stabilizing effect of radioactive tracer is presumed to be

TABLE 1. Effect of organism and suspending medium on physical aerosol recovery of lyophilized bacteria

Organism ^a	Per cent in aerosol ^b
<i>Bacillus subtilis</i> var. <i>niger</i> /DW	2.1 (0.1)
<i>B. subtilis</i> var. <i>niger</i> /SCS	3.6 (1.6)
LVS/SCS/ ¹⁴ C	3.0 (1.4)
<i>Escherichia coli</i> /DW/ ¹⁴ C	17.8 (5.5)
<i>E. aerogenes</i> /DW/ ¹⁴ C	19.5 (5.9)

^a DW = distilled water, SCS = spent culture supernatant from growing LVS, LVS = live vaccine strain *P. tularensis*, and ¹⁴C = carbon 14 tracer.

^b Aerosol cloud age at 2 min, normalized to the total lyophilized material in serum bottle before dissemination. Numbers in parentheses represent standard deviation of measurements.

related to an electrostatic discharge effect and appears to be offset if lyophilization involves spent culture supernatant as the suspending medium. The relative ranking of recoveries did not change during the course of a 30-min experiment.

In conclusion, it is suggested that the aerosol generator used in this paper provides a useful device for the dissemination of dry powders, particularly those for which pre-exposure to an atmosphere is to be either prevented or controlled. The efficiency with which the mass of powder in the serum bottle is disseminated as a small-particle-size aerosol varies with the nature of the material and is of a sufficient magnitude to allow studies of dry-fill-generated aerosols (2). Further, the particle-size selectivity associated with the interaction of lyophilized powder with both the disseminator and with the aerosol chamber, although producing losses, does result in physical stability of the residual aerosol. These physical losses have been attributed to electrostatic, inertial, and gravitational forces, and in part can be somewhat related to chamber design and technique. However, the types of losses encountered will be present to some extent in all lyophilized aerosol experimental systems utilizing a pneumatic dissemination technique and static aerosol chambers. Losses and aerosol physical stability particularly will be dependent on the nature of the bacterial suspending fluid used for freeze-drying and possibly on the species of organism and presence of a radioactive tag. The purely physical considerations of this study would apply equally well to aerosol investigations of inert particulate solids.

To obtain somewhat higher aerosol concentrations, the expedient of increasing the initial mass of dry material is perhaps feasible, since it is

unlikely that losses in the generator, including the serum bottle, increase in proportion to the initial amount of powder. However, since the coagulation rate of aerosol particles increases with increased particle concentration, an upper practical limit on concentration exists. Coagulation would have the effect of shifting the aerosol particle size distribution to a larger mean size with a concomitant acceleration of physical decay of the aerosol in a manner consistent with the model presented here.

ACKNOWLEDGMENTS

The authors acknowledge the contributions of Carroll L. Eicholtz for obtaining particle size analyses with the Micromerograph and Cameron Moffat for biological measurements. The authors are indebted to both for valuable assistance in experimental procedures.

LITERATURE CITED

1. Anderson, J. D., and C. S. Cox. 1967. Microbial survival. *Symp. Soc. Gen. Microbiol.* 17:203-226.
2. Cox, C. S. 1970. Aerosol survival of *Escherichia coli* B disseminated from the dry state. *Appl. Microbiol.* 19:604-607.
3. Derr, J. S., Jr. 1963. Models for deagglomeration and fracture of particulate solids, p. 227-263. *In* R. L. Dimmick (ed), A symposium on aerobiology. Naval Biological Laboratory, School of Public Health, Univ. of Calif., Naval Supply Center, Oakland.
4. Goldberg, L. J., H. M. S. Watkins, E. E. Burke, and M. A. Chatigny. 1958. The use of a rotating drum for the study of aerosols over extended periods of time. *Amer. J. Hyg.* 68:85-93.
5. May, K. R. 1945. The Cascade impactor: an instrument for sampling coarse aerosols. *J. Sci. Instrum.* 22:187-195.
6. May, K. R. 1964. Calibration of a modified Andersen bacterial aerosol sampler. *Appl. Microbiol.* 12:37-43.
7. May, K. R., and G. J. Harper. 1957. The efficiency of various liquid impinger samplers in bacterial aerosols. *Brit. J. Indust. Med.* 14:287-297.
8. Scaff, W. L., D. L. Dyer, and K. Mori. 1969. Fluorescent Europium chelate stain. *J. Bacteriol.* 98:246-248.
9. Zimmerman, L. 1962. Survival of *Serratia marcescens* after freeze-drying or aerosolization at unfavorable humidity. *J. Bacteriol.* 84:1297-1302.